Electrical Power Quality and Utilisation, Journal Vol. XVII, No. 2, 2014

A Study on the Low Frequency Transients in Power Transformers and Some Protection-Related Issues

Mohamed M. Said
IEEE Senior Member, Professor (Emeritus), Independent Researcher,
Giza, Cairo, Egypt, m.said@ieee.org, mmsaied2@yahoo.com

Summary:This paper presents typical results for the non-linear low frequency transients following the energization of power transformers. The three operating conditions of no-load, full-load and internal faults are considered. A direct analytical procedure is applied for solving the corresponding set of differential equations describing the transformers equivalent circuit. The core representation is based on the use of curve fitting applied to their magnetization curves. The results include plots versus time for the supply current, the core flux, the magnetizing current as well as the internal induced voltage. Moreover, graphs for the hysteresis loops relating the instantaneous values of both the excitation current and the core flux are given. An approach is also presented for the numerical determination of the amplitudes of the different harmonics existing in any of these signals utilizing the corresponding equidistant samples. As examples, the DC offset as well as harmonics up to the fourth order are considered. It is shown that several useful features can be extracted from the results in both the time and harmonic domains that can assist in differentiating between overcurrents resulting from short-circuits or inrush phenomena.

Key Words:
Transformer cores,
Inrush current,
Protection, transients,
Modeling,
Equivalent circuit,
Low frequency,
Nonlinear model,
Simulation

1. INTRODUCTION:

The possibility of the false tripping of transformer protection due to the relatively high inrush current following the energization at no load has attracted the attention of numerous researchers such as [1–17]. They report on investigations dealing with the analysis and simulation of the inrush current phenomena in power transformers and substations as well as their impact on the design and operation of the protective schemes. The time-domain and frequency-domain analyses are the two main approaches currently applied for finding the transient performance of power transformers [1–3, 4, 6, 7, 11, 12, 15–17]. The frequency- (or, equivalently, the s-domain) approach assumes problem's linearity, a fact that seriously limits the applicability of this approach. The time-domain methods, on the other hand, can deal with nonlinear issues such as core saturation, ferro-resonance and inrush phenomena. For instance, in [1], the Ewart's model was chosen for studying the over-voltages resulting from the non-vertical chopping of the transformer magnetizing currents. Furthermore, the strongly distorted current, voltage and flux wave forms appearing in systems are also reported on.

In terms of transformers' protection, reference [16] addresses procedures such as voltage- or harmonic-current-constraints being used in order to distinguish between large fault currents (for which the fast disconnection of the transformer is necessary) and eventually excessive magnetizing inrush currents (for which the protection should not operate). The reference also investigates the inrush current phenomena in substations including parallel-connected transformers or transformer banks, referred to as sympathetic interaction or switching. They deal with the determination of the interesting signals (i.e. currents, fluxes and voltages) of each transformer, the total substation current and the common bus voltage. The effect of shunt power factor correcting capacitors are also investigated.

Reference [15] suggests a procedure for the discrimination between situations involving internal faults and those of inrush currents in power transformers. The procedure is based on the use of the current and voltage samples, together with the easily available data describing the transformer's magnetization curve. It estimates the numerical value of a fictitious equivalent resistance whose possible range is between zero and the value of the transformer's resistance in its no-load equivalent circuit. It is shown that too small values of this estimated resistance imply internal faults, whereas higher numerical values describe situations involving inrush currents. For the same purpose, reference [6] deals with the transformer differential protection augmented by a new discriminating approach based on the Wavelet transform and Fuzzy inference system using a Matlab/Simulink program.

This paper is an additional contribution to this topic. It is composed of three parts:

1. The results of applying a *Mathematica* program for simulating the transformer's low frequency switching transients are presented. The procedure will be validated, and its applicability to the normal loading, internal faults as well as to inrush current transients is demonstrated.
2. In the second part, a procedure is suggested and implemented for the digital determination of the zero-frequency offset and the different harmonics included in the relevant signals such as the supply current and the core flux.
3. Based on the presented time-domain results and on the harmonic spectra of the considered signals, criteria will be proposed that can help distinguish between fault and inrush conditions.

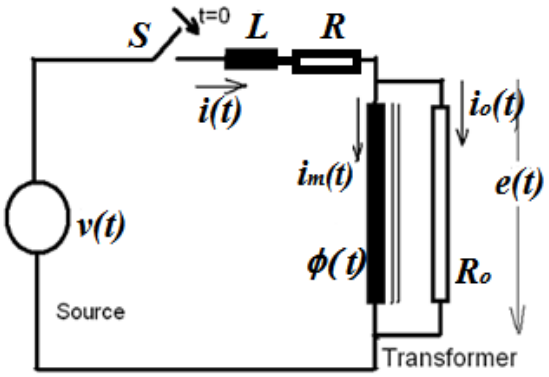

Fig.1. The assumed transformer equivalent circuit for analyzing the energization transient.

Part One: Simulation Technique of Transformer Energization Transients:

The Time-Domain Transient Analysis:

Figure 1 shows the equivalent circuit for the switching of a power transformer to the supply via the switch S which is closed at the time point $t = 0$. It depicts the voltage source $v(t)$, the leakage inductance L and the ohmic resistance R of the primary circuit. The figure shows also the instantaneous core flux $\varphi(t)$, magnetizing current $i_m(t)$ and the internally induced EMF $e(t)$. The resistance R_o and its associated current $i_o(t)$ are simulating the core losses. The transformer terminal current is denoted $i(t)$.

In order to describe the strongly nonlinear function relating the core flux $\varphi(t)$ to the corresponding exciting current $i_m(t)$, the following equation is assumed [14–16]:

$$\varphi(t) = a.\tan^{-1}[i_m(t)/c] + b.i_m(t) \qquad (1)$$

where a, b, c are transformer constants. They can be easily found using curve fitting techniques applied to the core magnetization curve.

The governing equations are

$$v(t) = V_{\max}\sin(\omega t + \alpha) = e(t) + L.i'(t) + R.i(t) \qquad (2)$$

$$e(t) = \phi'(t) \qquad (3)$$

$$i(t) = i_m(t) + e(t)/R_o \qquad (4)$$

where ω is the power angular frequency, and the phase angle α describes the switching time point relative to the supply voltage waveform.

Using the *Mathematica* package, a program was written for analytically solving the simultaneous differential and algebraic equations (2), (3) and (4). It was then possible to determine the time wave forms of the three currents $i_m(t)$, $i_o(t)$, $i(t)$, the induced EMF $e(t)$ as well as the core flux $\varphi(t)$.

Part Two: Determination of The Harmonic Content:

Assuming that a time signal $f(t)$ is approximated by the expression

$$f(t) = F_0 + F_{1,\max}\sin(\omega t + \theta_1) + F_{2,\max}\sin(2\omega t + \theta_2) + \\ + F_{3,\max}\sin(3\omega t + \theta_3) + F_{4,\max}\sin(4\omega t + \theta_4) + ... \qquad (5)$$

with F_0, $F_{1,\max}$, $F_{2,\max}$, $F_{3,\max}$, $F_{4,\max}$ denoting the amplitudes, and θ_1, θ_2, θ_3, θ_4 are the corresponding phase angles. ω is the supply fundamental angular frequency in radians/sec.

Using a sampling interval of h seconds, the corresponding expression of the k^{th} sampled signal is

$$f(k) = F_0 + F_{1,\max}\sin(\omega k h + \theta_1) + F_{2,\max}\sin(2\omega k h + \theta_2) + \\ + F_{3,\max}\sin(3\omega k h + \theta_3) + F_{4,\max}\sin(4\omega k h + \theta_4) + ... \qquad (6)$$

The interval h in seconds is defined by

$$h = 1/(N.SupplyFrequency) \qquad (7)$$

and N is the number of samples per power frequency cycle.

The accuracy increases with the assumed number of terms included in the equation (5). The zero-frequency (offset), the fundamental component and the harmonics of the second, third and fourth order were found sufficiently accurate in dealing with the here addressed case studies. Under these circumstances, and with known sampling interval h and angular power frequency ω, nine quantities are required in order to describe the assumed series $f(k)$. They are F_0, $F_{1,\max}$, $F_{2,\max}$, $F_{3,\max}$, $F_{4,\max}$ and θ_1, θ_2, θ_3, θ_4, for which nine equations are needed. The first equation describes the known samples of the function, denoted $f_0(k)$. The eight other equations are available from finding the first, second,…,eighth time derivatives, i.e. $f_1(k)$, $f_2(k)$, $f_3(k)$ and $f_4(k)$, respectively. It can be proved that these derivatives are related by

$$f_m(k) = [f_{(m-1)}(k+1) - f_{(m-1)}(k-1)]/2 \qquad (8)$$

with m assuming the values 1,2,3,…….,8.

The estimated amplitude of the zero-frequency component is then given by equation 9 (next page), whereas the amplitude of the fundamental component is equation 10.

Similarly, the maximum values of the second, third and fourth harmonic of the signal $f(t)$ are available from the three following equations 11, 12, and 13.

The Data of the Considered Transformer:

The plot in Figure 2 illustrates the relation between the per unit magnetizing current i_m and the per unit core flux φ. The base values are 9.6 A and 0.99 Wb, respectively. The dots are measurements of a 3 kVA, single-phase transformer adopted from [3]. The continuous line is the result of the curve fitting using *Mathematica*, yielding:

$$\phi/0.99 = 0.037171(i_m/9.6) + 1.087174\tan^{-1}(i_m/9.6) \qquad (14)$$

$$F_0 = \frac{576h^8\omega^8 \mathrm{f0}(k) + 620h^6\omega^6 \mathrm{f2}(k) + 273h^4\omega^4 \mathrm{f4}(k) + 30h^2\omega^2 \mathrm{f6}(k) + \mathrm{f8}(k)}{576h^8\omega^8} \tag{9}$$

$$F_{1,\max} = -\frac{1}{360\sqrt{h^{16}\omega^{16}}}\sqrt{16\,h^8\omega^8\left\{17568\,h^4\omega^4 \mathrm{f1}(k)\,\mathrm{f3}(k) + 20736\,h^6\omega^6 \mathrm{f1}(k)^2 + 17568\,h^2\omega^2 \mathrm{f2}(k)\,\mathrm{f4}(k) + \right.}$$
$$\sqrt{\left. 20736h^4\omega^4 \mathrm{f2}(k)^2 + 3721\left[h^2\omega^2 \mathrm{f3}(k)^2 + \mathrm{f4}(k)^2\right]\right\} + 2h^4\omega^4 \mathrm{f7}(k)\left[576h^4\omega^4 \mathrm{f1}(k) + \right.}$$
$$\sqrt{\left. 244h^2\omega^2 \mathrm{f3}(k) + 29\mathrm{f5}(k)\right] + 232h^8\omega^8 \mathrm{f5}(k)\left[144h^2\omega^2 \mathrm{f1}(k) + 61\mathrm{f3}(k)\right] + } \tag{10}$$
$$\sqrt{2h^2\omega^2 \mathrm{f8}(k)\left[576h^4\omega^4 \mathrm{f2}(k) + 244h^2\omega^2 \mathrm{f4}(k) + 29\mathrm{f6}(k)\right] + 232h^6\omega^6 \mathrm{f6}(k)\left[144h^2\omega^2 \mathrm{f2}(k) + 61\mathrm{f4}(k)\right] + }$$
$$\sqrt{841h^6\omega^6 \mathrm{f5}(k)^2 + 841h^4\omega^4 \mathrm{f6}(k)^2 + h^2\omega^2 \mathrm{f7}(k)^2 + \mathrm{f8}(k)^2}$$

$$F_{2,\max} = -\frac{1}{720\sqrt{h^{16}\omega^{16}}}\sqrt{1152\,h^8\omega^8 \mathrm{f1}(k)\left[169\,h^4\omega^4 \mathrm{f3}(k) + 26\,h^2\omega^2 \mathrm{f5}(k) + \mathrm{f7}(k)\right] + 82944h^{14}\omega^{14} \mathrm{f1}(k)^2 + }$$
$$\sqrt{2h^2\omega^2 \mathrm{f8}(k)\left[144h^4\omega^4 \mathrm{f2}(k) + 169h^2\omega^2 \mathrm{f4}(k) + 26\mathrm{f6}(k)\right] + 3744h^8\omega^8 \mathrm{f2}(k)\left[13h^2\omega^2 \mathrm{f4}(k) + 2\mathrm{f6}(k)\right] + }$$
$$\sqrt{20736h^{12}\omega^{12} \mathrm{f2}(k)^2 + 169h^4\omega^4\left[208h^4\omega^4 \mathrm{f3}(k)\,\mathrm{f5}(k) + 676h^6\omega^6 \mathrm{f3}(k)^2 + 52h^2\omega^2 \mathrm{f4}(k)\,\mathrm{f6}(k) + \right.} \tag{11}$$
$$\sqrt{\left. 169h^4\omega^4 \mathrm{f4}(k)^2 + 16h^2\omega^2 \mathrm{f5}(k)^2 + 4\mathrm{f6}(k)^2\right] + 104h^4\omega^4 \mathrm{f7}(k)\left[13h^2\omega^2 \mathrm{f3}(k) + 2\mathrm{f5}(k)\right] + 4h^2\omega^2 \mathrm{f7}(k)^2 + \mathrm{f8}(k)^2}$$

$$F_{3,\max} = -\frac{1}{2520\sqrt{h^{16}\omega^{16}}}\sqrt{1152\,h^8\omega^8 \mathrm{f1}(k)\left[84\,h^4\omega^4 \mathrm{f3}(k) + 21\,h^2\omega^2 \mathrm{f5}(k) + \mathrm{f7}(k)\right] + 36864h^{14}\omega^{14} \mathrm{f1}(k)^2 + }$$
$$\sqrt{128h^6\omega^6 \mathrm{f2}(k)\left[84h^4\omega^4 \mathrm{f4}(k) + 21h^2\omega^2 \mathrm{f6}(k) + \mathrm{f8}(k)\right] + 4096h^{12}\omega^{12} \mathrm{f2}(k)^2 + } \tag{12}$$
$$\sqrt{9h^2\omega^2\left\{49h^2\omega^2\left[72h^4\omega^4 \mathrm{f3}(k)\,\mathrm{f5}(k) + 144h^6\omega^6 \mathrm{f3}(k)^2 + 8h^2\omega^2 \mathrm{f4}(k)\,\mathrm{f6}(k) + 16h^4\omega^4 \mathrm{f4}(k)^2 + 9h^2\omega^2 \mathrm{f5}(k)^2 + \mathrm{f6}(k)^2\right] + \right.}$$
$$\sqrt{\left. 42h^2\omega^2 \mathrm{f7}(k)\left[4h^2\omega^2 \mathrm{f3}(k) + \mathrm{f5}(k)\right] + \mathrm{f7}(k)^2\right\} + 42h^2\omega^2 \mathrm{f8}(k)\left[4h^2\omega^2 \mathrm{f4}(k) + \mathrm{f6}(k)\right] + \mathrm{f8}(k)^2}$$

$$F_{4,\max} = -\frac{1}{20160\sqrt{h^{16}\omega^{16}}}\sqrt{1152\,h^8\omega^8 \mathrm{f1}(k)\left[49\,h^4\omega^4 \mathrm{f3}(k) + 14\,h^2\omega^2 \mathrm{f5}(k) + \mathrm{f7}(k)\right] + 20736h^{14}\omega^{14} \mathrm{f1}(k)^2 + }$$
$$\sqrt{2h^2\omega^2 \mathrm{f8}(k)\left[36h^4\omega^4 \mathrm{f2}(k) + 49h^2\omega^2 \mathrm{f4}(k) + 14\mathrm{f6}(k)\right] + 504h^8\omega^8 \mathrm{f2}(k)\left[7h^2\omega^2 \mathrm{f4}(k) + 2\mathrm{f6}(k)\right] + }$$
$$\sqrt{1296h^{12}\omega^{12} \mathrm{f2}(k)^2 + 49h^4\omega^4\left[448h^4\omega^4 \mathrm{f3}(k)\,\mathrm{f5}(k) + 784h^6\omega^6 \mathrm{f3}(k)^2 + \right.} \tag{13}$$
$$\sqrt{\left. 28h^2\omega^2 \mathrm{f4}(k)\,\mathrm{f6}(k) + 49h^4\omega^4 \mathrm{f4}(k)^2 + 64h^2\omega^2 \mathrm{f5}(k)^2 + 4\mathrm{f6}(k)^2\right] + }$$
$$\sqrt{244h^4\omega^4 \mathrm{f7}(k)\left[7h^2\omega^2 \mathrm{f3}(k) + 2\mathrm{f5}(k)\right] + 16h^2\omega^2 \mathrm{f7}(k)^2 + \mathrm{f8}(k)^2}$$

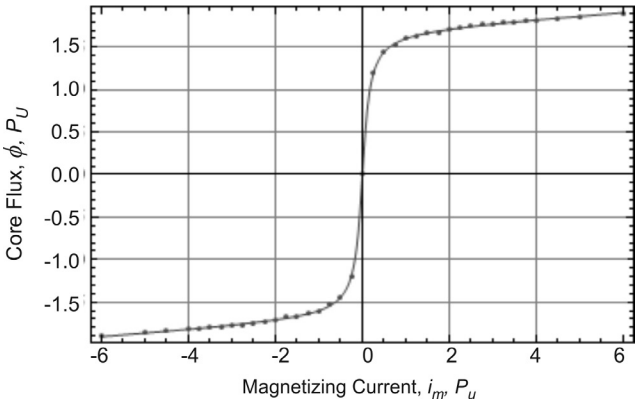

Fig. 2. The assumed saturation curve. The dots represent measurements adopted from [3]

The remaining data of this transformer are:

Rated primary voltage	311.1 V
Rated frequency	50 Hz
Per unit primary resistance	0.003673
Per unit primary reactance	0.001390
Per unit iron loss	0.0365364

The results below are for a voltage switching angle of $\alpha = 0$, as defined by equation (2).

Part Three: Sample Results:

The Supply Current *i*(*t*):

The plots of Figure 3 depict the time response of the supply current in A following the energization of the above mentioned transformer. The three following conditions are considered: fully-loaded (resistive), short-circuited and open-circuited transformer secondary. The results are given in Figs. 3-(a), 3-(b) and 3-(c), respectively. In each figure, the graph to the left is the waveform over the first 500 milliseconds (i.e. 25 cycles), whereas the one to the right illustrates the current wave after 246 cycles (i.e. almost steady-state).

Addressing the case of fully loaded transformer, the peak value (around 14 A) of the slightly distorted almost pure sinusoidal steady state current, Plot 3-(a)-right, agrees well with the previously assumed rated (base) current of 9.6 A (rms). This case exhibits a considerable transient component immediately after energization. Both plots pertinent to the case (b) of the transformer's short circuit show an almost pure sinusoidal current wave having the constant amplitude of approximately 3200 A. This value agrees with the expected value $311.1\sqrt{2}/\sqrt{0.003673^2 + 0.00139^2}$ A, from the assumed transformer series circuit parameters and the supply voltage. The inrush current of the third case (c) dealing with the energization of the unloaded transformer is always positive for the value $\alpha = 0$ of the source voltage. The corresponding strongly distorted steady state magnetizing current is illustrated by the Plot 3-(c)- right. It is in full agreement with the current given in [3] measured during a no load test of the transformer.

The supply current $i(t)$ is sampled at a rate of 24 samples / cycle, and substituted in Eqs. (8) through (13) in order to get the harmonic distributions in the above three operating conditions. It should be noted that no estimates can be made before the arrival of the ninth sample, i.e. $k \geq 9$.

Table (I-A). Estimated Harmonics in the Supply Current $i(t)$, Peak Values (Initial Distribution, $k = 9$)

Transformer's Operating Condition	DC Offset, A	Fundamental Component	Second Harmonic	Third Harmonic	Fourth Harmonic
Full Load	42	170	75	18.5	3.6
Short Circuit	210	3000	110	28	3.0
Open Circuit	41	167	76	18.5	3.6

Table (I-B). Estimated Harmonics in the Supply Current $i(t)$, Peak Values (Final Distribution, $k = 1500$)

Transformer's Operating Condition	DC Offset, A	Fundamental Component	Second Harmonic	Third Harmonic	Fourth Harmonic
Full Load	1.5	14	2	1.5	0.2
Short Circuit	0	3250	17	2.7	0.2
Open Circuit	1.5	5	2	1.5	0.2

Table (I-A) lists the first estimate of frequency spectrum of the supply current at $k = 9$. The DC offset, the amplitudes fundamental component as well as the second, third and fourth harmonics. There is no much difference between the values corresponding to the full loading and the energization of the unloaded transformer in this regard. All five components of the supply current under short circuit conditions are generally larger than those of the two other cases. Although the second harmonic current of 110 A is the largest among the three cases, it constitutes only 3.67% of the fundamental component. In the case of switching the unloaded transformer, the second harmonic amplitude is over 45.5% of the fundamental current. Table (I-B) shows the components of the supply current after the arrival of 1500 samples (i.e . 1.25 seconds). The given values are computed using the latest data window of 9 samples. As expected, the DC current offset, the third as well as the fourth harmonic current decrease considerably. In particular, the zero frequency current offset approaches zero under short circuit conditions. The second harmonic components in percent of the fundamental current for the three cases of full load, short circuit and no load switching are approximately 14%, 0.52% and 45.5%, respectively. This indicates the possibility of using the percentage second harmonic current as a reliable criterion for the discrimination between short circuit faults and inrush currents.

The Induced EMF *e*(*t*):

The plots in Figure 4 (a), (b) and (c) depict the time wave forms of the induced EMF $e(t)$ in the three cases of resistive full load, short circuit fault and no load switching, respectively. No major decaying zero-frequency components (offset) can be recognized in the three cases. It can be further seen that, apart from the slightly higher harmonic content in case (c), there are apparently no significant differences between the corresponding initial and steady-state wave

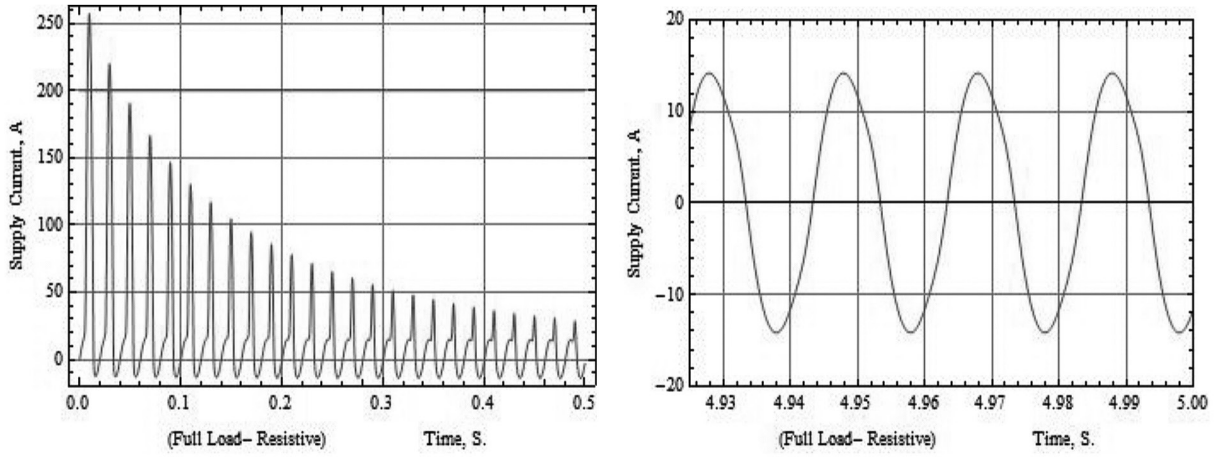

(a) Transformer fully loaded at unity power factor

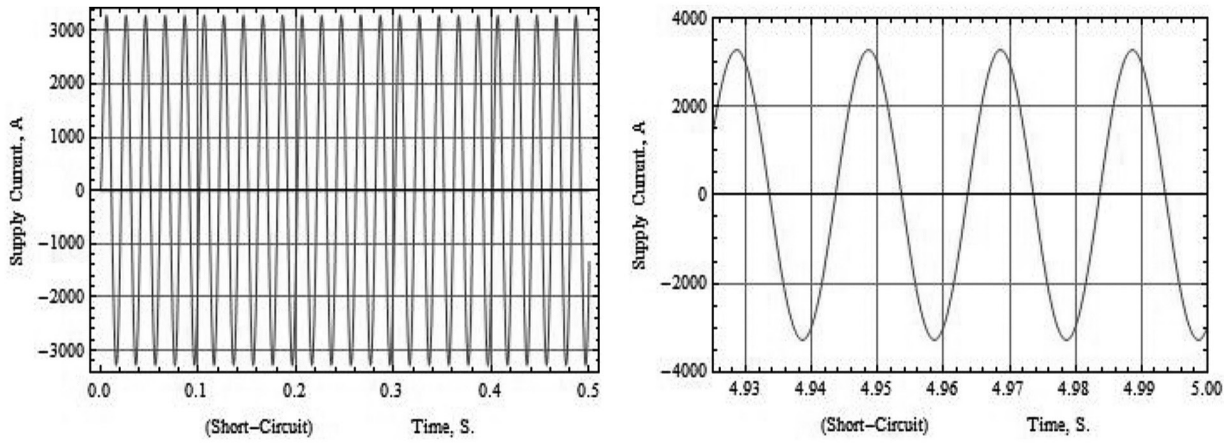

(b) Transformer is short-circuited

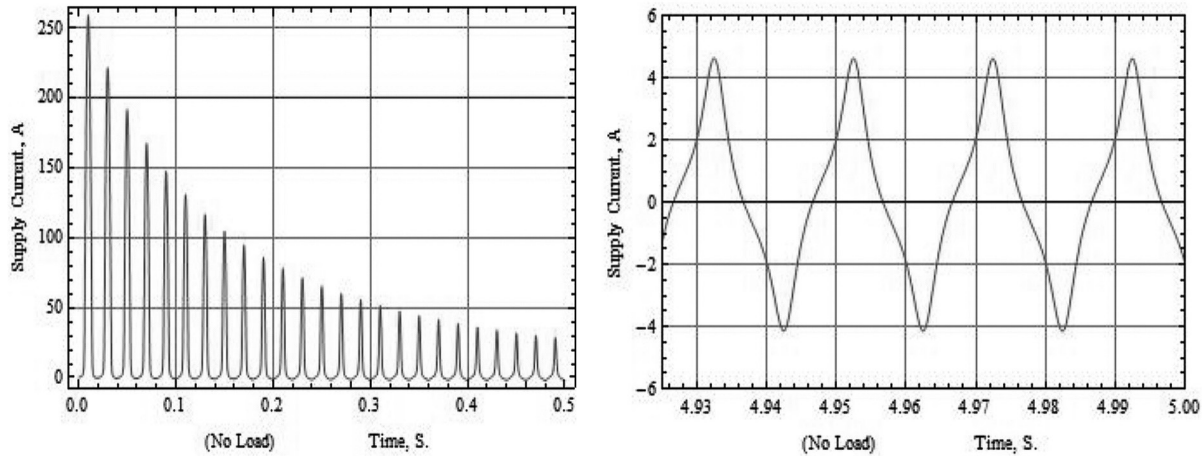

(c) Transformer open-circuited

Fig. 3. The transients over the first 500 milliseconds (left), and the steady state wave forms (right) of the supply currents $i(t)$ under the three operating conditions.

forms in the two cases of energizing the transformer under full load or no-load condition. In both cases (a) and (c), the peak value of the alternating component of the EMF is approximately 425 V. On the other hand, the corresponding value for the more linear case of energizing the short-circuited transformer, (b), is about 26 V.

The above results imply that the transformer's induced EMF $e(t)$ represents a reliable criterion for differentiating between internal short circuits and inrush transients. This is especially important in situations where the transformer is energized from a power network of a high short circuit level,

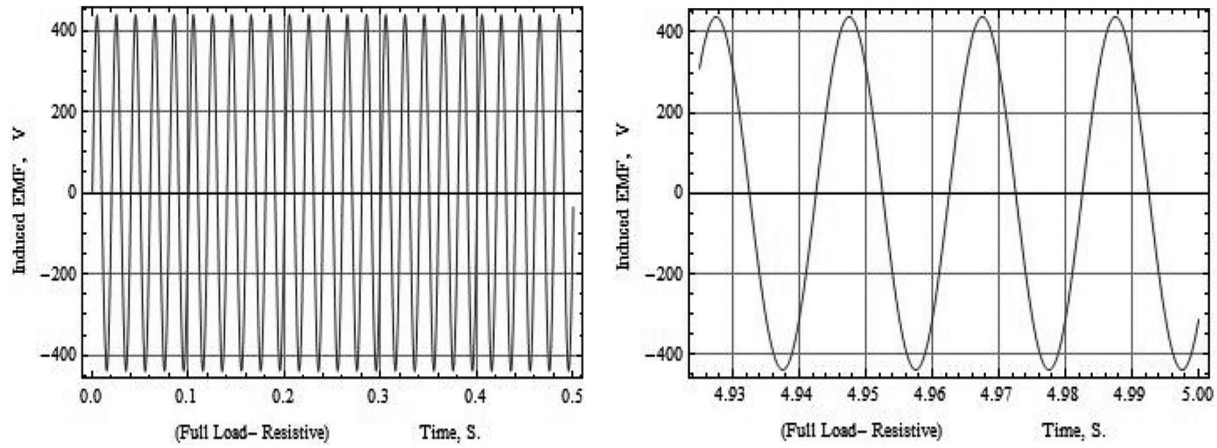

The Induced EMF $e(t)$:

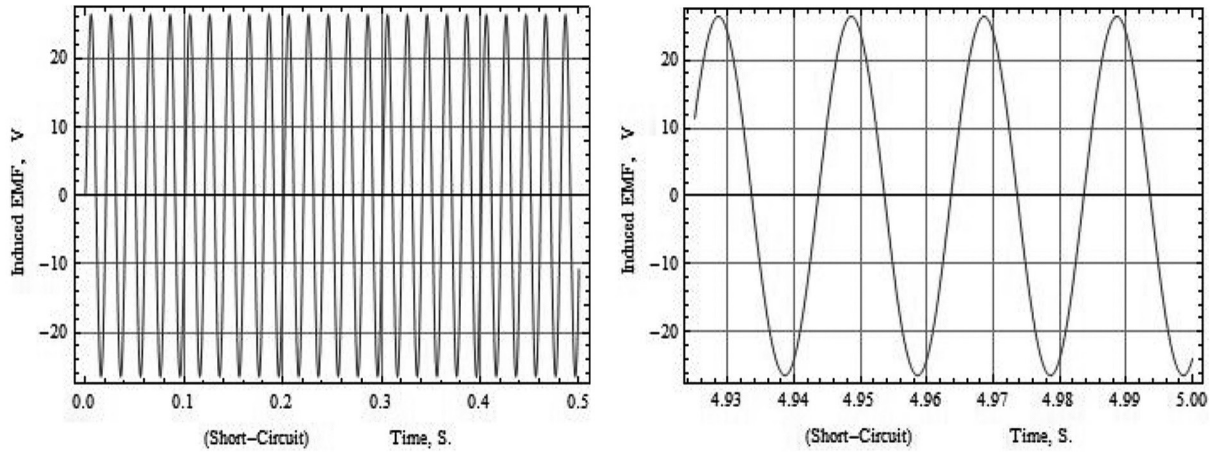

(a) Transformer fully loaded at unity power factor

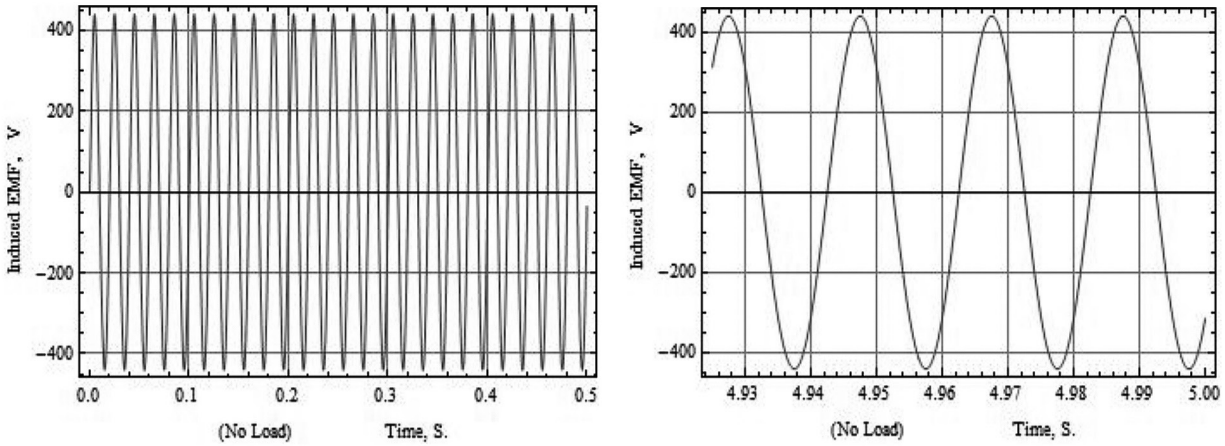

(b) Transformer is short-circuited

(c) Transformer is open-circuited

Fig. 4. The transients over the first 500 milliseconds (left), and the steady state wave forms (right) of the induced EMF $e(t)$

resulting in a transformer terminal voltage (during internal faults) which is close to the rated value.

The Core Flux $\varphi(t)$:

Under ideal sinusoidal conditions, and if the transformer's primary impedance is neglected, the peak value of the core flux is Weber. This agrees with the amplitudes of the steady state flux wave forms pertinent to the two cases (a) and (c) in Figure 5. The case (b) describing the conditions for internal fault are characterized by a small flux amplitude (approximately 0.085 Weber). This lies within the linear range of the core flux. In all the three case studies (a), (b) and (c), there is a complete zero-frequency (DC) offset in the flux

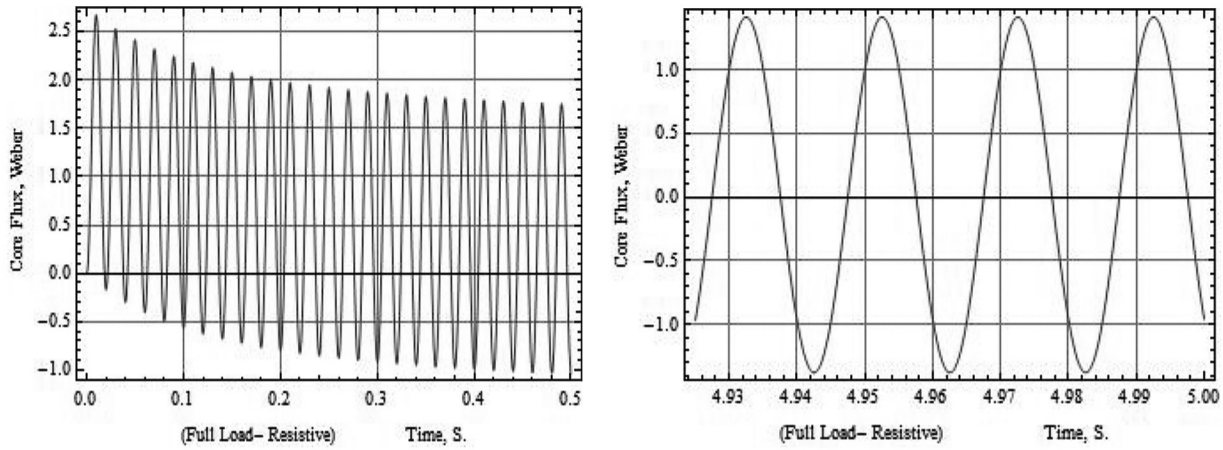

(a) Transformer fully loaded at unity power factor

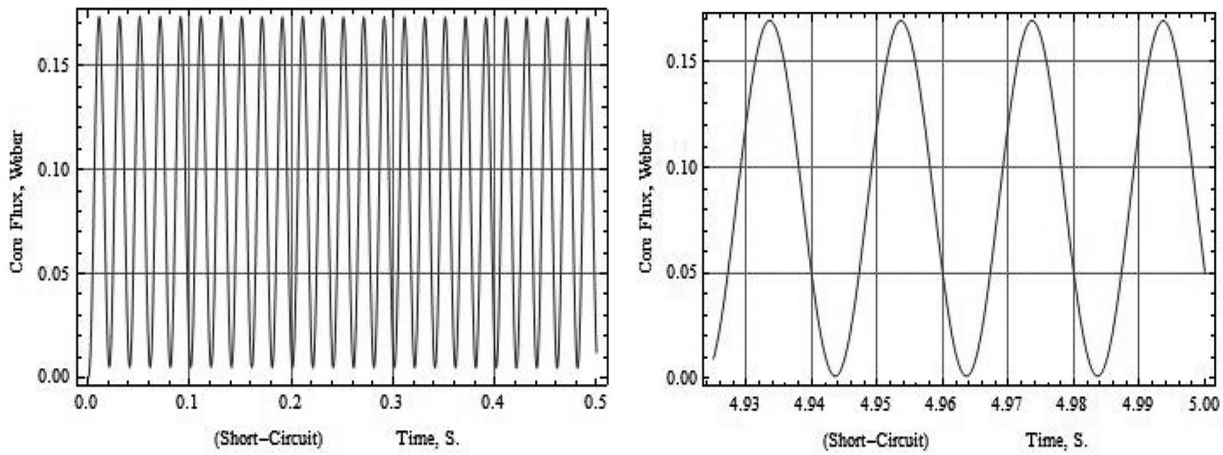

(b) Transformer is short-circuited

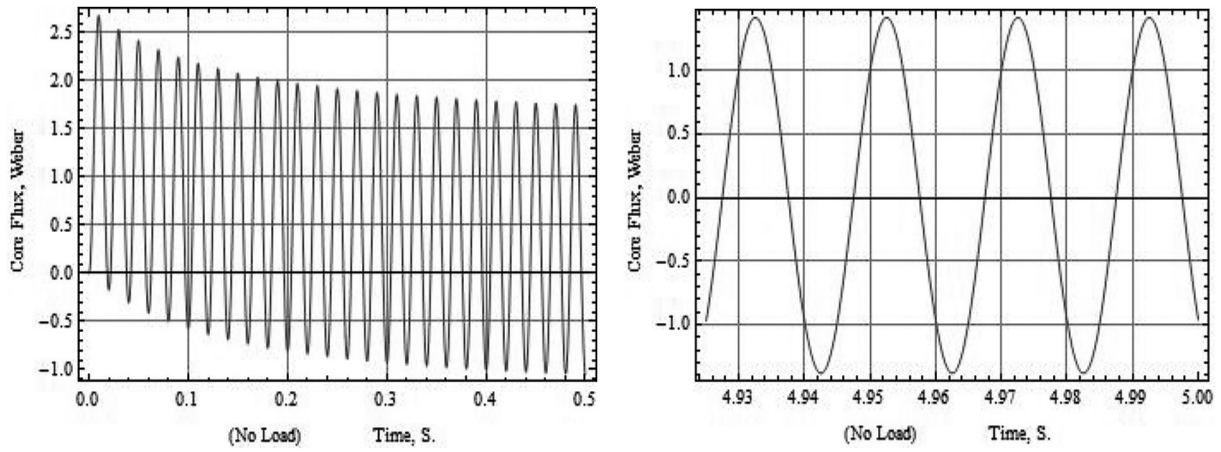

(c) Transformer is open-circuited

Fig. 5. The transients over the first 500 milliseconds (left), and the steady state wave forms (right) of the core flux $\varphi(t)$.

wave forms. Fig.5 indicates that the decay of the offset core flux is very slow in the case (b) describing the transformer transients under short circuit condition. This can be attributed to the relatively small core losses due to the reduced flux.

The Transformer's Magnetization Loops:

The plots (a), (b) and (c) in Fig.6 show the magnetization loops corresponding to the cases of energizing the transformer in the three cases of full resistive load, short circuit and open

Table (II-A). Estimated Harmonics in the Induced EMF $e(t)$, Peak Values (Initial Distribution, $k=9$).

Transformer's Operating Condition	DC Offset, A	Fundame ntal Component	Second Harmonic	Third Harmonic	Fourth Harmonic
Full Load	21	437	12	≥4	≥1.2
Short Circuit	1.5	26.0	0.90	0.26	0.025
Open Circuit	22	438	11.6	2.7	0.90

Table (II-B). Estimated Harmonics in the Induced EMF $e(t)$, Peak Values (Final Distribution, $k=1500$).

Transformer's Operating Condition	DC Offset, A	Fundame ntal Component	Second Harmonic	Third Harmonic	Fourth Harmonic
Full Load	0	435	2.2	0.5	0.1
Short Circuit	0	26.0	0.15	0.022	0.0018
Open Circuit	0	437	2.50	0.50	0.10

Table (III-A). Estimated Harmonics in the Core Flux $\varphi(t)$, Peak Values (in milli Weber)
(Initial Distribution, $k=9$).

Transformer's Operating Condition	DC Offset, A	Fundame ntal Component	Second Harmonic	Third Harmonic	Fourth Harmonic
Full Load	1400	1420	15	2.58	0.57
Short Circuit	89.4	85.5	1.4	0.30	0.03
Open Circuit	1350	1420	15	4.5	0.6

Table (III-B). Estimated Harmonics in the Core Flux $\varphi(t)$, Peak Values (in milli Weber)
(Final Distribution, $k=1500$).

Transformer's Operating Condition	DC Offset, A	Fundame ntal Component	Second Harmonic	Third Harmonic	Fourth Harmonic
Full Load	200	1385	7.50	1.0	0.120
Short Circuit	88.3	83.7	0.07	0.07	0.006
Open Circuit	150	1393	7.50	1.0	0.120

circuited secondary, respectively. In terms of Mathematica, they are the parametric plots of the instantaneous values of the total shunt current $i_o(t)+e(t)/R_o$ in Fig.1 and the core flux $\varphi(t)$ over the time range from zero to 0.5 second.

It can be observed that the two plots (a) and (c) are almost identical. The current values oscillate between -4 A and a value greater than +12 A, while the core flux excursions are between -1.4Wb and +1.6 Wb. The graph in Fig.6-(b) illustrates the transformer's magnetization curve under short circuit conditions. The magnetizing current varies between the two limits zero and +0.21 A whereas the corresponding values of the core flux are zero and +0.175 Wb, respectively. The plot is pretty much of a smooth elliptic shape, because the transformer does not go into saturation. The area of each of the parametric plots of Fig.6 is equal to the core energy lost per cycle.

Table (IV-A). Estimated Harmonics in the Supply Current $i(t)$, in Percent of the Fundamental Component
(Initial Distribution, $k=9$).

Transformer's Operating Condition	Fundamental Component [%]	Second Harmonic Component [%]	Third Harmonic Component [%]	Fourth Harmonic Component [%]
Short Circuit	100	3.67	0.93	0.1
Open Circuit	100	45.5	11.1	2.16

Table (IV-B). Estimated Harmonics in the Induced EMF $e(t)$, in Percent of the Fundamental Component
(Initial Distribution, $k=9$).

Transformer's Operating Condition	Fundamental Component [%]	Second Harmonic Component [%]	Third Harmonic Component [%]	Fourth Harmonic Component [%]
Short Circuit	100	3.46	1	0.096
Open Circuit	100	2.65	0.616	0.205

Protection-Related Issues

This section addresses some considerations regarding the reliable protection of power transformers. Special attention will be paid to the discrimination between the high currents due to internal faults and the inrush currents resulting from energizing the unloaded transformers. The signals typically available for transformer protection are the terminal voltage and the input current. According to Fig.1, $e(t)$ can be easily obtained from the samples of the terminal voltage $v(t)$ and the instantaneous voltage drop across the primary side resistance R and inductance L. The inductive voltage drop will require the numerical computation of the first derivative of the current $di(t)/dt$. This can be accomplished through the application of Eq.(8), i.e. $i'(k) = [i(k+1) - i(k-1)]/2h$. The following discussion will accordingly focus on the use of the terminal current $i(t)$ as well as the EMF $e(t)$. The two tables Table (IV-A) and Table (IV-B) present the amplitudes of the 2nd, 3rd and the 4th harmonics of both the current and the EMF in percent of the corresponding fundamental components which were listed earlier in Tables (III-A) and (III-B). Table (IV-A) indicates that the harmonic content in the supply current is more than ten times higher in the case of no-load transformer switching. This suggests that the percentage second order harmonic current (rather than the

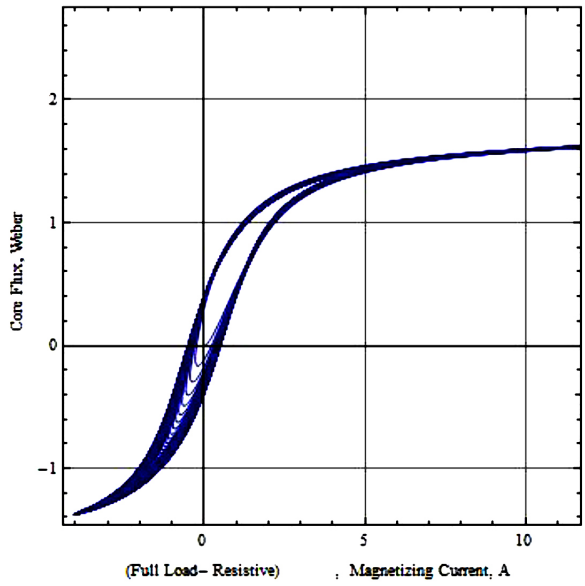

(a)

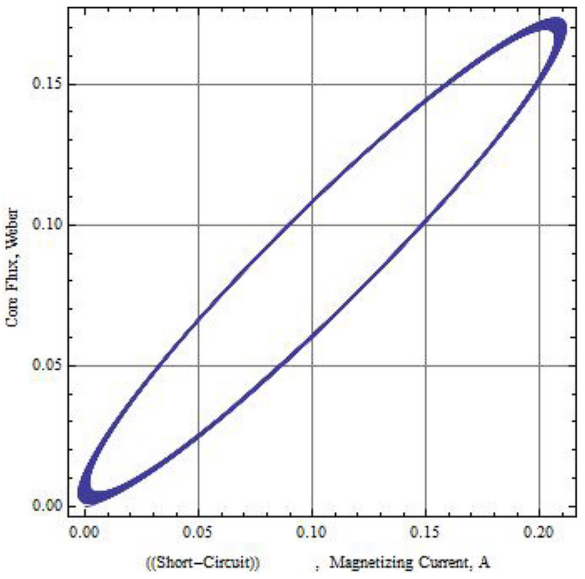

(b)

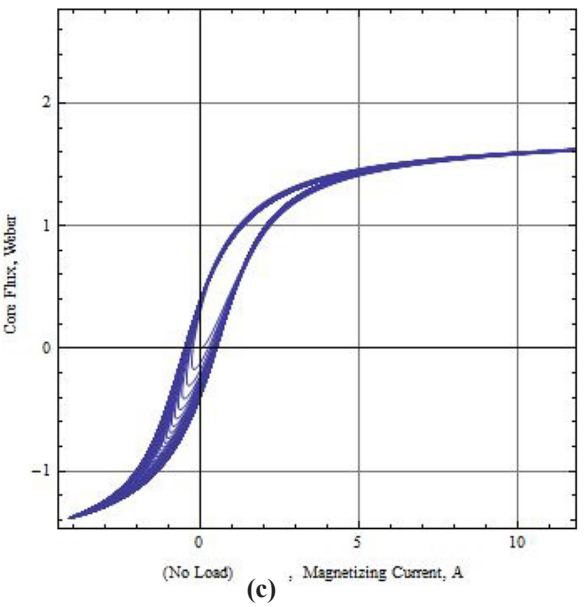

(c)

Fig. 6. The transformer's core magnetization loops over the first 500 milliseconds.

cases of internal short-circuit and current inrush in no-load energization, respectively.

According to the results in Table (IV-B) of the induced EMF e(t), there is no significant difference between the two cases of short circuit or open circuit switching in terms of the percentage harmonic content in the three considered EMF harmonic components.

3. CONCLUSIONS

1. Typical non-linear low frequency energization transients of power transformers under different operating conditions are investigated. The core representation is based on the use of curve fitting applied to their magnetization curves.
2. The presented results include the supply and magnetizing currents, the core flux, the induced EMF and the hysteresis loop relating the instantaneous values of both the excitation current and the flux.
3. An approach is proposed for the numerical determination of the amplitudes of the different harmonics existing in any of the above signals utilizing the corresponding equidistant samples. As examples, the DC offset and the harmonics up to the fourth order are considered.
4. It is shown that several useful features can be extracted from the results in both the time and harmonic domains that can assist in distinguishing between fault and inrush conditions.
5. The second harmonic current in percent of the fundamental for the three cases of full load, short circuit and no load switching are approximately 14%, 0.52% and 45.5%, respectively. This indicates the possibility of using the percentage second harmonic current for the reliable discrimination between short circuit faults and inrush currents.
6. Apart from the slightly higher harmonic content in the case of energization under no-load, there are no significant differences between the corresponding initial and steady-state wave forms in the two cases of switching the transformer under full load or no-load condition.
7. The results show that the transformer's induced EMF represents a reliable criterion for differentiating between internal short circuits and inrush transients.
8. The decay of the offset core flux with time is very slow in the case describing the transients under short circuit condition. This can be attributed to the relatively small core losses due to the reduced flux.
9. The magnetization loops in the two cases of full load and open circuit energization are almost identical. Due to the absence of saturation, the loop resulting from the energization under short-circuit exhibits a smooth elliptic shape.
10. The results indicate that the harmonic content in the supply current is more than ten times higher in the case of no-load switching. This implies that the percentage second harmonic current (rather than the absolute values) can be reliably used for the differentiation between these two situations.

REFERENCES:

1. Abdul-Rahman Kh.H., Saied M.M.: On the Exact Computation of Some Typical Transient and Dynamic Phenomena in Power Networks Including Iron-core Transformer. Proc. of the IEEE Industrial and Commercial Power Systems Conference, IEEE Industry Applications Society, Irvine, California, USA, April 25 - May 2, 1994
2. Baoming G., Almeida A., Qionglin Z., Xiangheng W.: An Equivalent Instantaneous Inductance-Based Technique for Discrimination between Inrush Current and Internal Faults in Power Transformer. IEEE Transactions On Power Delivery, Vol. 20 (2005), Iss. 4, pp. 2473-2482
3. Bogarra S., Font A., Candela I., Pedra J.: Parameter estimation of a transformer with saturation using inrush measurements. Electric Power Systems Research, Vol. 79 (2009), Iss. 2, pp. 417-425
4. Bronziado H.S., Brogan P.B., Yacamini R.: Harmonic Analysis of Transient Currents during Sympathetic Interaction. IEEE Transactions on Power Systems, Vol. 11 (1996), Iss. 4, pp. 2051-2056
5. Computer Relaying. IEEE Tutorial Course Text No. 79EH0148-7-PWR, The IEEE Power Engineering Society
6. Ghania S.M.: Internal Faults/In-Rush Currents Discrimination Based on Fuzzy/Wavelet Transform in Power Transformers. International Journal of Electrical and Power Engineering, Vol. 6 (2012), Iss. 3, pp. 100-110
7. Greenwood A.: Electrical Transients in Power Systems. Second Edition. Wiley-Interscience 1991, Chapters 5&12
8. Gross C.A.: Power System Analysis. Second Edition. John Wiley & Sons, New York 1986, Chapter 11
9. Lucas J.R., McLaren P.G.: B-H Loop Representation for Transient Studies. Intl. Journal of Electrical Engineering Education (IJEEE), Vol. 28 (1991), No. 3, pp. 261-270
10. Makky A-R. A.: Representation of Magnetization Curves. Paper No. A78054-9 presented at the IEEE PES Winter Meeting, New York, Jan. 29-Feb. 3, 1978
11. Makky A-R. A.: Sympathetic Interaction between Loaded Transformers Caused by Inrush Phenomenon. Proc. of the Sixth Middle East Power Conference (MEPCON'98), Egypt, Dec. 15-17, 1998, pp. 119-123
12. Martinez J.A., Mork B.A.: Transformer Modeling for Simulation of Low Frequency Transients. Proc. of the Power Engineering Society General Meeting, Vol. 2, Toronto, July 13-17, 2003
13. Mason C.R.: The Art and Science of Protective Relaying. John Wiley, New York 1956
14. Perez-Rojas C.: Fitting Saturation and Hysteresis via Arctangent Functions. IEEE Power Engineering Review, Vol. 20 (2000), Iss. 11, pp. 55-57
15. Saied M.: A Method for Distinguishing Between Faults and Inrush Phenomena in Power Transformers. Proc. of the 2007 International Conference on Advanced Power System Automation and Protection, APAP2007-485, April 24-27, 2007, Jeju, Korea
16. Saied M.: A Study on the Inrush Current Phenomena in Transformer Substations. Proc. of the 36th Annual Meeting of the IEEE Industry Applications Society, Paper P-28-3, pp. 1180-1187, Chicago IL, October 2001
17. Wiechowski W., Bak-Jensen B., Leth Bak C., Lykkegaard J.: Harmonic Domain Modeling of Transformer Core Nonlinearities Using DigSilent Power Factory Software. Electric Power Quality and Utilisation Journal, Vol. 14 (2008), Iss. 1, pp. 3-11

Mohamed Mostafa Saied

Received the B.Sc. degree (Honors) in Electrical Engineering from Cairo University, Egypt in 1965, then the Dipl.-Ing. and Dr-Ing. degrees from RWTH Aachen, Germany, in 1970 and 1974. From 1974 to 1983, he was at Assiut University, Egypt. In 1983, he joined Kuwait University where he served as full professor and EE Department Chairman. He spent one-year sabbatical leave (1998) as a Visiting Professor at Cairo University. Since his retirement in 2009, Prof. Saied. Works as an Independent Researcher, Giza, Cairo, Egypt. He is an IEEE Senior Member since 1984.